

# A mixed-addenda Mo/W organofunctionalized hybrid polyoxometalate

Sharad S. Amin,<sup>a</sup> Jamie. M. Cameron,<sup>a</sup> Max Winslow,<sup>b</sup> E. Stephen Davies,<sup>c</sup> Stephen P. Argent,<sup>c</sup> David Robinson,<sup>b</sup> and Graham. N. Newton<sup>a\*</sup>

[a] Dr. S. S. Amin, Dr. J. M. Cameron and Dr. G. N. Newton  
Nottingham Applied Materials and Interfaces (NAMI) Group  
School of Chemistry  
University of Nottingham  
Nottingham, NG7 2TU, UK  
E-mail: Graham.Newton@nottingham.ac.uk

[b] Mr. M. Winslow and Dr. D. Robinson  
Department of Chemistry and Forensics  
Nottingham Trent University  
Clifton Lane, Nottingham, NG11 8NS, UK

[c] Dr. E. S. Davies and Dr. S. Argent  
School of Chemistry  
University of Nottingham  
University Park, Nottingham NG7 2RD, UK

**Abstract:** A mixed-addenda W/Mo hybrid polyoxometalate cluster -  $K_6[P_2W_{15}Mo_2O_{61}(POC_6H_5)_2]$  (**1**) was synthesized from the condensation of  $K_{10}[P_2W_{15}Mo_2O_{61}]$  and  $PO_3C_6H_7$  under acidic conditions. Single-crystal X-ray diffraction confirmed the structure of the hybrid cluster and the presence of two Mo centers in the cap of the lacunary cluster. The electronic effects of metal substitution were studied by cyclic voltammetry, spectroelectrochemistry and electron paramagnetic resonance spectroscopy and supported by density functional theory calculations. Comparing **1** to its tungsten-only analogue  $K_6[P_2W_{17}O_{61}(POC_6H_5)_2]$  (**2**), a more positive potential for the first reduction process was induced by the substitution of W for Mo, consistent with a significant lowering of the cluster LUMO energy.

of medicine,<sup>7</sup> molecular electronics<sup>8,9</sup> and catalysis.<sup>10</sup> In recent years, however, more consideration has been given to the preparation and characterisation of hybrid POMs,<sup>5, 11</sup> owing to their highly tuneable properties, including visible-light photoactivity,<sup>12</sup> supramolecular self-assembly,<sup>13-16</sup> and redox chemistry.<sup>17, 18</sup> The combined benefits of addenda metal ion substitution and organo-functionalisation are likely to offer greater scope to tune the physical properties of the POM cluster,<sup>19</sup> however, the preparation of such systems is synthetically challenging and only a handful of mixed-metal hybrid POMs have been reported. The primary examples are the  $\{W_{15}V_3\}$  tungstovanadate hybrids,<sup>20</sup> "tris"-functionalised hetero-metal centred Anderson hybrids<sup>21</sup> and more recently, lanthanide substituted polyphosphotungstates.<sup>22</sup>

## Introduction

Polyoxometalates (POMs) are a class of polynuclear anionic molecular metal-oxide clusters, consisting of early transition metals (i.e. W, Mo, V etc.) in their highest oxidation states. These nanoscopic clusters are well-known for their rich and reversible redox chemistry, stability and tuneability. Their synthesis involves the pH-controlled condensation of metal oxide fragments which can be driven to self-assemble into a range of structure types, each of which exhibit unique physical properties. Their stability and photo/redox activity has seen them employed in several fields including biochemistry,<sup>1</sup> energy storage,<sup>2</sup> and photocatalysis.<sup>3, 4</sup>

Under mildly basic conditions partial hydrolysis of POM clusters can be achieved, yielding lacunary structures which can be readily modified by either: i) complexation of transition metal ions to yield transition metal-substituted POMs (TM-POMs), or; ii) binding of main-group elements tethered to organic moieties, forming so-called organic-inorganic hybrid POMs (hybrid POMs). Both strategies profoundly impact the physical and chemical properties of the POM cluster.<sup>5, 6</sup> Much of the early work on the modification of lacunary POMs focussed on TM-POMs and found them to exhibit a range of potential applications across the fields

The synergistic impact of incorporating mixed-metal centres into redox- and photo-active organophosphonate hybrid POMs remains unexplored despite offering a promising pathway to further enhance their properties (e.g. visible-light photoresponsiveness). Herein, we report the preparation of an organophosphonate hybrid POM based on a mixed-metal Wells-Dawson lacunary structure,  $K_{10}[P_2W_{15}Mo_2O_{61}]$   $\{W_{15}Mo_2\}$ ,<sup>23</sup> and investigate the effects of Mo substitution on the electronic properties of the hybrid cluster with respect to its mono-metallic polyoxotungstate analogue.

## Results and Discussion

The lacunary cluster was synthesised from an existing methodology published by Contant *et al.*,<sup>23</sup> following which, phenyl phosphonic acid was appended to the cluster via an acid mediated condensation reaction to afford  $K_6[P_2W_{15}Mo_2O_{61}(P_2O_2C_6H_5)]$  (**1**). This molecule was structurally characterised by synchrotron XRD, NMR, MS, and UV-Vis. Further experimental details can be found in the SI.

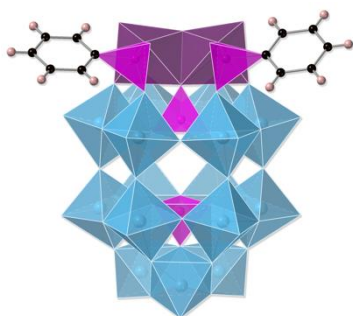


**Figure 1.** Crystal structure of **1** with solvent molecules and cations removed for clarity. Two Mo addenda are located in the upper cap of the Wells-Dawson cluster which are covalently bound to organophosphonates. Colour scheme: blue polyhedra are  $\{WO_6\}$ , magenta polyhedra are  $\{PO_4\}$ , and plum polyhedra are  $\{MoO_6\}$  units. Carbon and hydrogen centres are black and light pink respectively.

Single crystals of **1** were obtained by vapor diffusion of MeOH into a saturated solution of **1** in MeCN to yield pale green single crystals. **1** was analysed by synchrotron X-ray diffraction and was found to crystallise in the monoclinic space group  $P2_1/n$ . A full description of the crystallographic data collection and refinement can be found in the supporting information (Table S2). The structure of the polyoxoanion, **1**, consists of two phenylphosphonic acid moieties covalently grafted onto the  $\{W_{15}Mo_2\}$  cluster in a 2:1 fashion in a manner analogous to previously reported isostructural phenylphosphonate hybrid polyoxotungstate, **2**.<sup>24</sup> The single crystal refinement unambiguously confirms the position of the Mo atoms to be localised in the capping site of the cluster. <sup>31</sup>P NMR (Figure S1) also clearly shows three distinct P environments, which supports the assignment of the Mo addenda to the cap positions (*i.e.* no scrambling was observed on the timeframe of the measurement).

To probe the effects of Mo substitution on the electronic structure of **1**, cyclic voltammetry (CV) and UV/vis spectroelectrochemical analysis was conducted (Figures 2 & 3) and these results were compared to the tungsten-only analogue,  $K_6[P_2W_{17}O_{61}(POC_6H_5)_2]$  (**2**), which was prepared using a previously reported method.<sup>24</sup> CV measurements were recorded in DMF with 0.1 M [TBA][PF<sub>6</sub>] supporting electrolyte (Figure 2) and are reported at a scan rate of 100 mV/s over a potential range of 0 to -2.5 V vs. Fc<sup>+</sup>/Fc. CV analysis in this potential range shows a series of closely overlapping redox processes for both **1** and **2**. Square wave voltammetry (SWV) (Figure S3b) was conducted on each hybrid to better resolve the potentials of these reductions. The presence of Mo-centres in **1** results in a significantly more positive potential of the first redox process relative to **2**, indicating an overall lowering in energy of the LUMO due to the substitution of Mo addenda into the cluster. Common POM addenda atoms can be ordered in terms of decreasing oxidizing ability as follows: V(V) > Mo(VI) > W(VI).<sup>25,26</sup> Therefore, in the case of one-electron reduced mixed-addenda POMs, the electron is expected to be localized on the more readily reduced metal centre.<sup>25</sup> In this instance, we expect for the single e<sup>-</sup> on the reduced POM to be associated with the reduction of a Mo<sup>VI</sup> centre. To explore this, UV/vis absorption spectroelectrochemistry and electron paramagnetic resonance (EPR) spectroscopy were employed (Figure 3).

Typically, the addenda ions in POMs possess a d<sup>0</sup> electronic configuration, resulting in a large feature in the UV-vis absorption spectrum located between 190 and 400 nm and ascribed to an oxygen-to-metal charge transfer transition (LMCT).<sup>26</sup> The spectra associated with reduced POMs exhibits characteristic intervalence charge transfer bands associated with inter-valence charge transfer (IVCT) between metal centres.<sup>27,28</sup> By employing spectroelectrochemical analysis, it is possible to distinguish between the reduction of different addenda when comparing compounds with different compositions (*i.e.* Mo and W). In Figures 3a & c, the growth of the IVCT bands was followed as increasingly negative potentials were applied to the system, details of which are included in the SI. For each data point, the potential was held until the IVCT absorption band remained unchanged between successive scans, indicating that all POMs in solution had been reduced at the applied potential. The absorption spectrum collected after the first reduction of **1** to **[1]**<sup>-</sup> displayed a very broad feature with a peak around 800-900 nm. In contrast, the spectrum associated with **[2]**<sup>-</sup> exhibits a broad IVCT band with distinct  $\lambda_{max} = 837$  nm. The clear difference in the absorption profiles for the singly reduced states of both **[1]**<sup>-</sup> and **[2]**<sup>-</sup> is therefore a good initial indicator that the first reduction process in **1** is at least partially localised to the molybdenum centres.

Spectral changes associated with the second, third and fourth (for **1** only) reductions were also followed by UV/vis spectroelectrochemistry and for each a blue shift was observed in the peak tops in the spectra of **1** relative to those in the spectra of **2**. The spectroelectrochemical data allows us to draw some qualitative conclusions about the system. The differences in the spectra of **1** and **2** suggest that the first reduction process exhibited by **1** is primarily Mo-centred. In contrast, the second yields a comparatively sharp peak that is reminiscent of that shown by **[2]**<sup>2-</sup>, albeit significantly blue-shifted (see the red traces in Figure 3a and c), suggesting the process is likely to be W-centred. The third reduction of **1** results in a low broad peak, reminiscent of the spectral changes induced by the first reduction

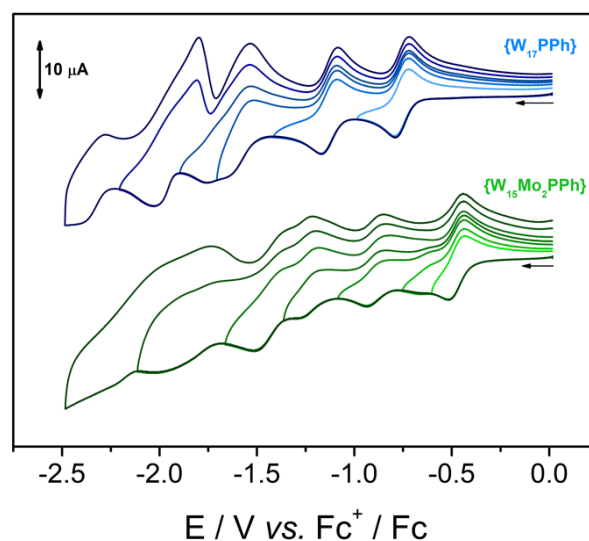


**Figure 2.** CV plots of **1** (green) and **2** (blue) conducted in DMF and 0.1 M [TBA][PF<sub>6</sub>] supporting electrolyte. Potentials reported against Fc<sup>+</sup>/Fc.

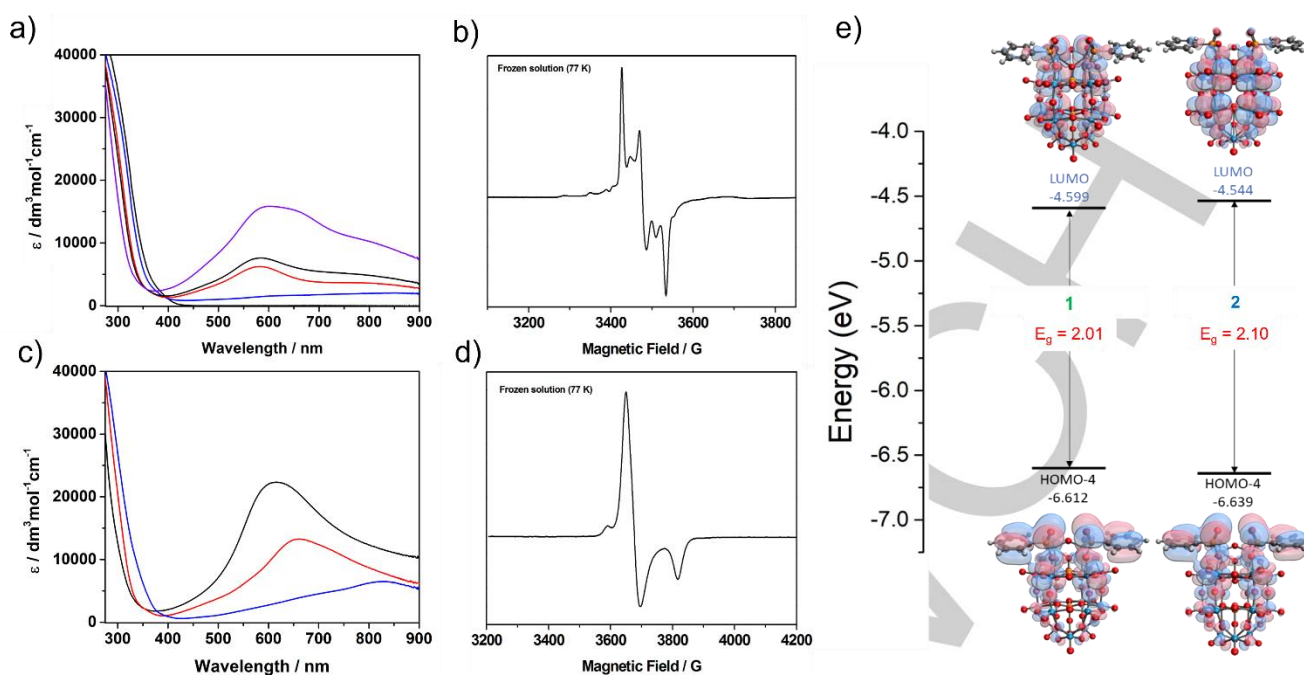


**Figure 3.** UV/Vis spectroelectrochemical analysis of a) **1** and c) **2** in DMF with 0.1 M [TBA][PF<sub>6</sub>] as supporting electrolyte where plots represent the UV/Vis absorption profile of POM reduced species produced by applying potential past the 1st (blue), 2nd (red), 3rd (black), and 4th (purple) reduction potentials (red arrows on SWV plot in Figure S2 show applied potentials); X-band EPR spectroscopy of the 1e<sup>-</sup> reduced species b) [**1**]<sup>-</sup> and d) [**2**]<sup>-</sup> in DMF with 0.1 M [TBA][PF<sub>6</sub>] as supporting electrolyte; e) DFT calculated HOMO-LUMO orbital diagram of **1** (left) and **2** (right) showing the calculated highest POM-centred HOMO and LUMO energies, and HOMO-LUMO energy gap (E<sub>g</sub>).

process of **1** and consistent with a Mo-centred redox event. We also note the significant differences between the corresponding peaks (black traces in Figure 3a and c) in the spectra of [**1**]<sup>3-</sup> and [**2**]<sup>3-</sup>, where the W-centred process in **2** leads to an intense, relatively sharp peak. The fourth reduction of **1** results in a similar peak change to those seen in **2**, hinting that it may be W-centred.

To further elucidate the location of the electron associated with the first 1e<sup>-</sup> reduction process, EPR spectroscopy was conducted on singly reduced species [**1**]<sup>-</sup> and [**2**]<sup>-</sup> (Figure 3b & d). Bulk electrolysis experiments performed on solutions of **1** and **2**, at applied potentials of -0.58 V and -0.94 V (vs. Fc<sup>+</sup>/Fc), respectively, indicate that the first reduction processes are one-electron in each case (Figures S3 & S4). Further details of the reduction process can be found in the SI. [**1**]<sup>-</sup> was found to be EPR active, both as fluid (Figure S6) and frozen solution. For [**2**]<sup>-</sup> an EPR spectrum was only observed as a frozen solution at 77 K. The 77 K spectra are clearly different; [**1**]<sup>-</sup> appears rhombic and displays a series of small features at low field consistent with the presence of Mo hyperfine coupling (Figure 3b) whilst [**2**]<sup>-</sup> appears essentially axial, with a low field feature ascribed to <sup>183</sup>W hyperfine coupling (14.31 %, I = 1/2).<sup>29,30</sup>

To further probe the electronic structure of the hybrid POMs, density functional theory (DFT) calculations were employed, allowing us to determine the frontier orbital energy levels of **1** and **2** (Figure 3e). The geometry of each molecule was optimised in a polarisable continuum based on the dielectric constant of DMF. Frontier orbitals with the highest POM-based orbital contributions are considered to be the HOMO and LUMO. Based on DFT calculations, **1** possesses a lower LUMO energy than **2**, in agreement with experimental data acquired when comparing the first reduction potentials for the two clusters (*vide supra*).

Furthermore, the LUMO orbital is more evenly distributed across the entire POM for **2** whereas the LUMO orbital of **1** has a distribution skewed towards the Mo centres. The distribution of LUMO electron density across the POM corroborates the experimental data, as IVCT is most likely to occur between similar neighbouring metal centres, which is most likely why there is a lower degree of LUMO orbital delocalisation across the **1** cluster. Moreover, E<sub>g</sub> is lower for **1**, in good agreement with literature values for Mo-based POMs.<sup>30</sup> We have established that the LUMO energies are lower for **1**, however, **1** also exhibits a higher HOMO energy which also contributes to the lower E<sub>g</sub> (2.01 eV) compared to **2** (2.10 eV). The HOMO energy is raised as a result of lower orbital mixing of LUMO energies due to the different nuclei present. Therefore, **2** exhibits larger orbital mixing, a higher degree of electron delocalisation and therefore a more stabilised (i.e. lower energy) HOMO.

## Conclusion

A mixed addenda (Mo/W) organofunctionalized hybrid polyoxometalate was prepared and compared to an all-tungsten analogue through a combination of single crystal structural determination, (spectro)electrochemical analysis and theoretical studies. Detailed electrochemical analyses found the mixed-metal hybrid system to exhibit numerous quasi-reversible redox processes associated with both Mo and W centres; determinations supported by both controlled-potential absorption spectroscopy and theoretical analyses. The combined effects of metal substitution (W→Mo), and the electron-withdrawing effects of phosphonate ligands were found to significantly impact the frontier orbital energies of the hybrid POM. This new example of



## RESEARCH ARTICLE

a stable, multi-redox active mixed-metal hybrid-POM species raises significant potential opportunities in the development of visible light photooxidation catalysts and tuneable energy materials.

## Experimental Section

Synthesis of  $K_6[P_2Mo_2W_{15}O_{61}(POC_6H_5)_2] - 1$ 

$K_{10}[P_2W_{15}Mo_2O_{61}]$  (0.25 g, 0.059 mmol), phenyl phosphonic acid (18 mg, 0.114 mmol), and 12 M HCl (50  $\mu$ L) was then added. The reaction mixture was then heated at 80 °C for 24 h, and after cooling to r.t., the reaction mixture was centrifuged, whereby the solution was filter off to give a green solution. Et<sub>2</sub>O was added to the solution and the resulting precipitate was centrifuged to collect the solid. The solid was sonicated in Et<sub>2</sub>O to give **1** as a green powder (0.164 g, 63.5 %). <sup>1</sup>H NMR (400 MHz, DMSO-*d*<sub>6</sub>)  $\delta$  8.00 – 7.91 (m, 2H), 7.53 – 7.42 (m, 3H); <sup>31</sup>P NMR (162 MHz, DMSO-*d*<sub>6</sub>)  $\delta$  14.27, -9.79, -12.93.

Synthesis of  $K_6[P_2W_{18}O_{61}(POC_6H_5)_2] - 2$ 

$K_{10}[P_2W_{17}O_{61}]$  (0.25 g, 0.057 mmol), phenyl phosphonic acid (18 mg, 0.114 mmol), and KCl (126 mg, 1.7 mmol) were suspended in MeCN, and 12 M HCl (100  $\mu$ L) was then added. The reaction mixture was then heated at 80 °C for 24 h, and after cooling to r.t., the reaction mixture was filtered to give a yellow solution. Subsequent centrifugation with Et<sub>2</sub>O, EtOH, and Et<sub>2</sub>O gave **2** as a yellow powder (0.150 g, 58 %). <sup>1</sup>H NMR (400 MHz, MeCN-*d*<sub>3</sub>)  $\delta$  8.15 (ddt, *J* = 14.2, 6.6, 1.6 Hz, 2H), 7.56 (ddt, *J* = 10.3, 6.3, 1.8 Hz, 3H); <sup>31</sup>P NMR (162 MHz, Acetonitrile-*d*<sub>3</sub>)  $\delta$  15.58, -11.12, -12.71.

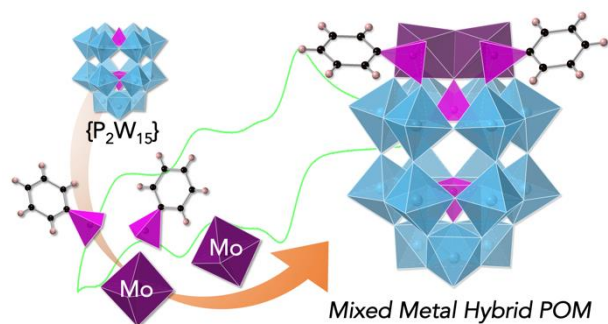
## Acknowledgements

The authors gratefully acknowledge the support of the EPSRC through the Centre for Doctoral Training in Sustainable Chemistry (EP/L015633/1) and the University of Nottingham Propulsion Futures Beacon of Excellence. GNN and JMC thank the Leverhulme Trust (RPG-2016-442). SSA thanks the EPSRC for the award of a Doctoral Prize.

**Keywords:** Polyoxometalate • mixed-metal cluster • hybrid materials • electrochemistry • spectroelectrochemistry

- [1] A. Bijelic, M. Aureliano and A. Rompel, *Chem. Comm.*, **2018**, 54, 1153-1169.
- [2] M. Genovese and K. Lian, *Curr Opin Solid State Mater Sci*, **2015**, 19, 126-137.
- [3] K. Suzuki, J. Jeong, K. Yamaguchi and N. Mizuno, *New J Chem*, **2016**, 40, 1014-1021.
- [4] X. B. Han, Z. M. Zhang, T. Zhang, Y. G. Li, W. Lin, W. You, Z. M. Su and E. B. Wang, *J. Am. Chem. Soc.*, **2014**, 136, 5359-5366.
- [5] A. J. Kibler and G. N. Newton, *Polyhedron*, **2018**, 154, 1-20.
- [6] J. E. Molinari, L. Nakka, T. Kim and I. E. Wachs, *ACS Catal.*, **2011**, 1, 1536-1548.
- [7] J. T. Rhule, C. L. Hill, D. A. Judd and R. F. Schinazi, *Chem. Rev.*, **1998**, 98, 327-358.
- [8] C. Boskovic, *Acc. Chem. Res.*, **2017**, 50, 2205-2214.
- [9] K. Y. Monakhov, M. Moors and P. Kögerler, *Adv. Inorg. Chem.*, Academic Press, **2017**, 69, 251-286.
- [10] C. L. Hill and C. M. Prosser-McCartha, *Coord. Chem. Rev.*, **1995**, 143, 407-455.
- [11] A. Dolbecq, E. Dumas, C. R. Mayer and P. Mialane, *Chem. Rev.*, **2010**, 110, 6009-6048.
- [12] J. M. Cameron, S. Fujimoto, K. Kastner, R. J. Wei, D. Robinson, V. Sans, G. N. Newton and H. H. Oshio, *Chem. Eur. J.*, **2017**, 23, 47-50.
- [13] E. Hampson, J. M. Cameron, S. Amin, J. Kyo, J. A. Watts, H. Oshio and G. N. Newton, *Angew. Chem. Int.*, **2019**, 58, 18281-18285.
- [14] S. Amin, J. M. Cameron, J. A. Watts, D. A. Walsh, V. Sans and G. N. Newton, *Mol. Syst. Des. Eng.*, **2019**, 4, 995-999.
- [15] K. Kastner, A. J. Kibler, E. Karjalainen, J. A. Fernandes, V. Sans and G. N. Newton, *J. Mater. Chem. A*, **2017**, 5, 11577-11581.
- [16] J. M. Cameron, G. Guillemot, T. Galambos, S. S. Amin, E. Hampson, K. Mall Haidaraly, G. N. Newton and G. Izzet, *Chemical Society Reviews*, **2022**, 51, 293-328.
- [17] C. L. Peake, A. J. Kibler, G. N. Newton and D. A. Walsh, *ACS Appl. Energy Mater.*, **2021**, 4, 8765-8773.
- [18] D. J. Wales, Q. Cao, K. Kastner, E. Karjalainen, G. N. Newton and V. Sans, *Adv. Mater.*, **2018**, 30, 1800159.
- [19] J. M. Cameron, S. Fujimoto, R.-J. Wei, G. N. Newton and H. Oshio, *Dalton Trans.*, **2018**, 47, 10590-10594.
- [20] D. Lachkar, D. Vilona, E. Dumont, M. Lelli and E. Lacôte, *Angew. Chem. Int.*, **2016**, 55, 5961-5965.
- [21] A. Blazevic, E. Al-Sayed, A. Roller, G. Giester and A. Rompel, *Chem. Eur. J.*, **2015**, 21, 4762-4771.
- [22] W. Wang, N. V. Izarova, J. van Leusen and P. Kögerler, *Chem. Comm.*, **2020**, 56, 14857-14860.
- [23] M. Abbessi, R. Contant, R. Thouvenot and G. Herve, *Inorg. Chem.*, **1991**, 30, 1695-1702.
- [24] S. Fujimoto, J. M. Cameron, R.-J. Wei, K. Kastner, D. Robinson, V. Sans, G. N. Newton and H. Oshio, *Inorg. Chem.*, **2017**, 56, 12169-12177.
- [25] M. Sadakane and E. Steckhan, *Chem. Rev.*, **1998**, 98, 219-238.
- [26] H. So and M. T. Pope, *Inorg. Chem.*, **1972**, 11, 1441-1443.
- [27] G. M. Varga, E. Papaconstantinou and M. T. Pope, *Inorg. Chem.*, **1970**, 9, 662-667.
- [28] M. B. Robin and P. Day, in *Advances in Inorganic Chemistry and Radiochemistry*, eds. H. J. Emeléus and A. G. Sharpe, Academic Press, **1968**, vol. 10, pp. 247-422.
- [29] R. R. Rakhimov, D. E. Jones, H. L. Rocha, A. I. Prokof'ev and A. I. Aleksandrov, *J. Phys. Chem. B*, **2000**, 104, 10973-10977.
- [30] L. Parent, P. A. Aparicio, P. de Oliveira, A.-L. Teillout, J. M. Poblet, X. López and I. M. Mbomekallé, *Inorg. Chem.*, **2014**, 53, 5941-5949.

## Entry for the Table of Contents



Substitution of metal addenda was explored as a method to modulate the electronic structure of organofunctionalized hybrid polyoxometalate clusters. Here we study the effects of Mo substitution into a W-based cluster. Through a range of spectroscopic and electrochemical techniques, substitution of W for Mo was shown to significantly modify the frontier orbital energies of the hybrid cluster.

Institute and/or researcher Twitter usernames: @DrGrahamNewton; @ChemistryUoN; @DrJamieCameron; @\_SharadAmin